Analytica Chimica Acta 1104 (2020) 188–198

Contents lists available at ScienceDirect

Analytica Chimica Acta

journal homepage: www.elsevier.com/locate/aca

Femtomolar direct voltammetric determination of circulating miRNAs in sera of cancer patients using an enzymeless biosensor

Mohamed Zouari [a, b], Susana Campuzano [c], José M. Pingarrón [c, d, **], Noureddine Raouafi [a, *]

[a] Sensors and Biosensors Group, Analytical Chemistry and Electrochemistry Lab (LR99ES15), Chemistry Department, University of Tunis El Manar, Tunis El Manar, 2092, Tunis, Tunisia
[b] Institut Pasteur de Tunis, 13 Place Pasteur, 1002, Tunis, Tunisia
[c] Departamento de Química Analítica, Facultad de CC. Químicas, Universidad Complutense de Madrid, E–28040, Madrid, Spain
[d] IMDEA Nanoscience, Ciudad Universitaria de Cantoblanco, 28049, Madrid, Spain

HIGHLIGHTS

- Enzymeless sandwich hybridization miRNAs biosensor at AuNPs/rGO/SPCEs.
- Fc-AuNPs-Strep as nanotracers for non-enzymatic labeling.
- Differential pulse voltammetric (DPV) measurement of the Fc oxidation peak.
- LOD of 5 fM, 2-months storage stability and single-mismatch discrimination.
- Accurate determination in 50 ng cellular RNA_t and diluted serum from cancer patients.

GRAPHICAL ABSTRACT

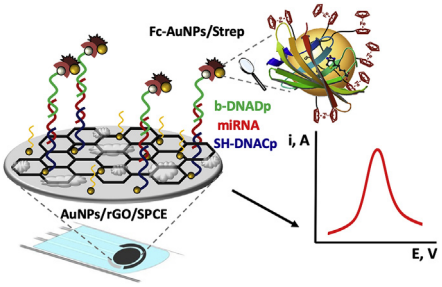

ARTICLE INFO

Article history:
Received 7 December 2019
Received in revised form
4 January 2020
Accepted 7 January 2020
Available online 15 January 2020

Keywords:
Breast cancer
Circulating miRNA–21
Graphene
Serum
Electrochemistry
Biosensor

ABSTRACT

A disposable enzyme–free biosensing platform for the sensitive and selective voltammetric determination of miRNAs is reported. The bioplatform implies a sandwich–type hybridization configuration involving the use of two synthetic DNA probes that hybridize contiguously with the target miRNA–21. A thiolated capture probe was immobilized through thiol chemistry on disposable carbon electrodes modified with a hybrid nanomaterial composed of reduced graphene oxide (rGO) and gold nanoparticles (AuNPs). A biotinylated detection probe was conjugated with ferrocene-capped AuNPs modified with streptavidin (Fc–AuNPs–Strep) which were used as labeling nanocarriers. The extent of the hybridization event was followed by differential pulse voltammetric measurement of the Fc oxidation peak. Under the optimized conditions, the developed biosensor provides attractive characteristics for the determination of the synthetic target miRNA, with a linear range between 10 fM and 2 pM and a limit of detection (LOD) of 5 fM, fully discrimination towards a highly homologous miRNA (with just one mismatched base) and a storage stability of at least two months. The biosensor was able to determine accurately the target miRNA directly in scarcely diluted serum from breast cancer (BC) patients with no need for a previous total RNA (RNA_t) extraction and in a very small amount of RNA_t extracted from breast

* Corresponding author.
** Corresponding author. Departamento de Química Analítica, Facultad de CC. Químicas, Universidad Complutense de Madrid, E–28040, Madrid, Spain.
E-mail addresses: pingarro@ucm.es (J.M. Pingarrón), noureddine.raouafi@fst.utm.tn (N. Raouafi).

https://doi.org/10.1016/j.aca.2020.01.016
0003-2670/© 2020 Elsevier B.V. All rights reserved.

adenocarcinoma cells without the need for amplification or reverse transcription to complementary DNA.

© 2020 Elsevier B.V. All rights reserved.

1. Introduction

Nowadays, high–throughput profiling/sensing of nucleic acids is a highly promising strategy for the early diagnosis and improved prognosis of a broad range of pathologies, most notably cancer. Among the candidate biomarkers with a great potential for this purpose are microRNAs (miRNAs), a class of endogenous non–coding RNAs of 19–25 nucleotides in length, of particular interest due to their role in the post–transcriptional regulation of gene expression [1]. Alterations in miRNA expression (either up– or down–regulation) are involved in the initiation and progression of human cancers, and characteristic miRNA expression profiles have been identified in specific types of cancers or pathogenic conditions. Indeed, the determination of tumor–derived miRNAs (circulating miRNAs) in biofluids such as serum, plasma, urine and saliva is emerging as novel fingerprints for human cancers detection, especially at early stage. Interestingly, these circulating miRNAs are extremely stable even in harsh pH conditions (from 1 to 13) and temperature (from freezing to boiling conditions) and are significantly more resistant to RNase activity than tissue or cellular miRNAs [1]. Therefore, the determination of miRNAs regulatory pattern is of great importance since it can provide relevant information about the type of tumor, its developmental stage of and/or its spreading potential, thus potentially transforming the way cancer is diagnosed and treated. However, their short sequence length, low natural abundance (typically femtomolar–picomolar level in clinical samples) [1] and structure and size homology of closely related non–target RNAs present in the clinical samples impose great challenges for their analysis [1–3].

In addition, the methods currently available for determination of miRNAs, including northern blot analysis, quantitative reverse transcription polymerase chain reaction (RT–qPCR), hybridization assays such as microarrays, and RNA sequencing, depend on sophisticated and costly laboratory instrumentation and are not suitable for miRNA biomarker screening in resource–limited settings [2,3]. Therefore, the development of alternative methodologies is of great interest. In this context, electrochemical biosensors have shown to provide important advantages against conventional strategies in terms of sensitivity, rapidity, simplicity, cost, amenability and portability [4]. They can be employed in scalable readout devices compatible with miniaturization, multiplexing and automation to perform accurate and on–site determinations of relevant biomarkers in clinical samples of highly variable complexity and nature [3]. These interesting features make them better meet the needs of current clinic and point–of–care (POC) disease evaluation.

A wide variety of electrochemical biosensing strategies have been proposed in connection with different enzyme–based nucleic acid amplification strategies (nuclease amplification [5], rolling circle amplification or RCA [6] and catalyzed hairpin assembly or CHA [7]). However, with the aim of facilitating their translation into routine clinical practice, there is an increasing tendency to develop nucleic acid amplification–free methods able to provide the required highly sensitive but are of simpler operation and do not need for previous reverse transcription of RNA to complementary DNA (cDNA). Some of the most attractive strategies described to date because of their simplicity, test time and excellent analytical performance involve: i) direct [8,9] or competitive [10,11], hybridization formats coupled with the use of nanomaterials or hybridization chain reaction and ii) hybridization of the target miRNA with synthetic DNA or RNA probes and capture/recognition of the resultant RNA hybrids regardless their sequence by bioreceptors with high specificity towards short (19–23 bp) RNA homohybrids (viral protein p19) [12] or RNA heterohybrids of any length (specific DNA–RNA antibodies) [13,14].

Interesting nucleic acid amplification–free methods achieving the required sensitivity were developed in combination with the use of nanomaterials due to their inherent advantages of biocompatibility, high catalytic properties, excellent conductivity and high loading capacity. In this context, mainly AuNPs, carbon nanomaterials and transition–metal dichalcogenides [2,3] have been used as tracers, catalysts, carriers of signaling tags [15,16], or electrode modifiers [10,17] to improve sensitivity. In addition, multiple amplification strategies using two or more types of nanomaterials and/or amplification methods can further enhance the analytical performance as well as offset the insufficiency of each individual component [17].

Graphene and its composites, especially with metal nanoparticles, have been widely used as electrode modifier in connection with enzyme biosensors [18,19] and immunosensors [20,21] due to inherent properties like large surface area for loading and good electrical conductivity. Moreover, the use of inorganic nanoparticles, such as quantum dots [22] and redox reporter capped metallic nanoparticles [16,23], as labels or labeling carriers provide an interesting way to develop enzyme–free methods less prone to poor reproducibility and even denaturation by temperature and pH variations.

Herein, we report the development of an enzyme–less sandwich hybridization–based electrochemical biosensor for the sensitive and selective determination of miRNAs (the oncomiR miRNA–21 was selected as a model target). The proposed approach relies for the first time on the smart combination of a sandwich hybridization assay implemented at screen–printed electrodes modified with nanohybrids of rGO with AuNPs (AuNPs/rGO) as scaffolds to immobilize a thiolated DNA capture probe and ferrocene-capped gold nanoparticles modified with streptavidin (Fc–AuNPs–Strep) as non–enzymatic tracers to conjugate the biotinylated DNA detector probe. It should be pointed here that the use of these Fc–AuNPs–Strep conjugates as nanocarriers of signaling elements have demonstrated to offer a very attractive alternative for amplification purposes in non-enzymatic based approaches due to the large number of redox moieties they carry mostly in connection with electrochemical biosensing of DNA [15,16,23] and scarcely for miRNAs and just in a magnetic-microbeads (MBs) based voltammetric assay [24] but no so far in integrated biosensing formats. Electrochemical detection was performed by DPV using Fc as redox reporter. The obtained results show the synergistic role of the individual nanomaterials in the hybrid nanocomposite to improve the performance of the developed biosensor achieving a high sensitivity for the synthetic target miRNA (LOD of 5 fM) and selectivity (single nucleotide discrimination). The biosensor was able to perform the accurate determination of miRNA–21 directly in scarcely diluted serum samples from cancer patients and a few amounts of cellular RNA_t (50 ng).

2. Materials and methods

2.1. Apparatus and electrodes

Cyclic voltammetry (CV), differential pulse voltammetry (DPV), chronoamperometry and electrochemical impedance spectroscopy (EIS) were performed with a Metrohm Autolab PGSTAT M204 electrochemical workstation using the Nova® v1.11 software. The transducers employed were screen–printed carbon electrodes (SPCEs, DRP–110 consisting of a 4–mm–diameter carbon working electrode, WE, a carbon counter electrode and an Ag pseudo–reference electrode). The SPCEs and the specific cable connector (DRP–CAC) to connect them with the potentiostat were purchased from Dropsens S.L (Oviedo, Spain).

A Bunsen AGT–9 Vortex for homogenization of the solutions, an ultrasonic bath Fisherbrand™, a Raypa steam sterilizer, a block heater (Stuart), a biological safety cabinet Telstar Biostar and a NanoDrop® ND–1000 spectrophotometer (NanoDrop Technologies) to evaluate the quality and quantity of the extracted cellular RNA was also employed.

The nanostructured electrode was characterized by scanning electron microscopy (SEM) using a field–emission scanning electron microscope JEOL JSM–7600 F.

2.2. Reagents and solutions

All reagents used were of the highest available grade. NaH_2PO_4, Na_2HPO_4, NaCl, $NaHCO_3$ and KCl were purchased from Scharlab (Spain). Tris–(hydroxymethyl)aminomethane hydrochloride (Tris–HCl), 6-mercaptohexanol (MCH), hydroquinone, H_2SO_4, tetrachloroauric acid trihydrate ($HAuCl_4 \cdot 3H_2O$), Na_2CO_3, H_2O_2 (30% w/v), ethylenediaminetetraacetic acid (EDTA), $K_4Fe(CN)_6$, $K_3Fe(CN)_6$, bovine serum albumin, 6–ferrocenylhexanethiol and streptavidin conjugated gold nanoparticles (Strep–AuNPs) were purchased from Sigma–Aldrich (Germany). Graphene oxide (GO) was purchased from Orion High Technologies (Spain).

All the buffer solutions used were prepared with Milli–Q water (18 MΩ cm at 25 °C) and sterilized after their preparation to avoid RNAse degradation. Buffer solutions used include: 0.1 M $NaHCO_3$/Na_2CO_3 buffer of pH 9.0; 0.01 M phosphate buffer solution containing 137.0 mM NaCl and 2.7 mM KCl (phosphate–buffered saline, PBS) of pH 7.5; 10 mM Tris–HCl supplemented with 1.0 mM EDTA and 0.3 M NaCl (Tris–EDTA buffer) of pH 8.0 and phosphate buffer 0.05 M of pH 6.0.

Other solutions/suspensions employed include: 1.0 mg mL^{-1} GO suspension prepared in 0.1 M $NaHCO_3$/Na_2CO_3 buffer solution (pH 9.0); a 5.0 mM $K_3Fe(CN)_6$/$K_4Fe(CN)_6$ solution supplemented with 0.1 M KCl; a 1 mM $HAuCl_4$ solution prepared in 0.5 M H_2SO_4.

Table 1 summarizes the nomenclature and the sequence of all the DNA and RNA synthetic oligonucleotides used. All these synthetic oligonucleotides, purchased from Sigma–Aldrich (Germany), were reconstituted upon their reception in nuclease–free water to a final concentration of 100 μM and stored at −80 °C into 5 μL–aliquots.

2.3. Preparation of Fc capped gold nanoparticle–streptavidin (Fc–AuNPs–Strep) conjugates

The AuNPs (diameter, 10 nm)/Strep conjugates were modified with 6–ferrocenylhexanethiol according to the protocol described by Wang et al. [15]. Firstly, 200 μL of the commercial conjugate solution were diluted to 400 μL with PBS buffer (pH 7.2). The resulting solution was mixed with 0.5 mL of hexane containing 5.0 mM 6–ferrocenylhexanethiol for 24 h on a vortex stirrer. The solution was centrifuged, and the hexane phase containing 6–ferrocenylhexanethiol was decanted. The AuNPs/Strep conjugates capped with 6–ferrocenylhexanethiol (Fc–AuNPs–Strep) were thoroughly rinsed with hexane and suspended in a PBS buffer (pH 7.2).

2.4. Preparation of the AuNPs/rGO/SPCE

SPCEs were activated by depositing a 50 μL–drop of PBS buffer (0.0 M) on the electrode surface and applying a constant potential of +1.7 V for 60 s. Thereafter, the electrode was washed with Milli–Q water and allowed drying in the air [26].

The activated WE was modified with rGO by electrodeposition using CV. GO was adsorbed on the WE surface during the oxidation scan and reduced in the reverse one. A 5 μL–drop of the 0.1 mg mL^{-1} GO suspension (previously sonicated in an ultrasonic bath up to homogeneity) was placed onto the WE and electrodeposited by scanning ten cyclic voltammograms between −0.5 and + 0.6 V (v = 50 mV s^{-1}) [27]. After this, the electrode was washed with Milli–Q water and allowed drying in the air.

AuNPs were electrodeposited on the rGO/SPCEs according to literature [28,29] by dropping 50 μL of the $HAuCl_4$ suspension and performing chronoamperometry at −0.5 V during 600 s. The AuNPs/rGO/SPCE was washed with Milli–Q water and allowed drying in the air.

The successful modification of SPCE with rGO and AuNPs was checked by SEM and CV of the bare SPCE, rGO/SPCE and AuNPs/rGO/SPCE resulting surfaces (see discussion and Fig. S1 in the Supporting Information).

2.5. Preparation of HS–DNACp–AuNPs/rGO/SPCE recognition interface

Immobilization of the HS–DNACp onto the modified SPCEs was carried out according to the protocol optimized with AuNPs/SPCEs [11–13]. In brief, a 10–μL aliquot of a 0.05 μM HS–DNACp solution (prepared in Tris–EDTA, pH 8.0) was dropped onto the WE and incubated for 8 h at 4 °C in a humidified chamber. After washing

Table 1
Oligonucleotides used in this work.

Oligonucleotide	Sequence (5′→3′)
Thiolated DNA capture probe (HS–DNACp)[a]	HS–$(CH_2)_3$–TCAACATCAGT
Biotinylated DNA detection probe (b–DNADp)[a]	CTGATAAGCTA–biotin
Target miRNA–21	UAGCUUAUCAGACUGAUGUUGA
1–mismatched miRNA–21 (1–m)	UAGCUUAUAAGACUGAUGUUGA
miRNA–451 (NC)[b]	UUGAGUCAUUACCAUUGCAAA

[a] To get the optimal hybridization yield in the sandwich hybridization assay, both HS–DNACp and b–DNADp (of 11 nucleotides (nts) each) were designed to hybridize contiguously with the 22 nts target miRNA–21, without non–hybridized nts gap between their hybridization sites [25].

[b] 1–m and NC: sequences with a different single–base (underlined) and fully non–complementary to the target miRNA.

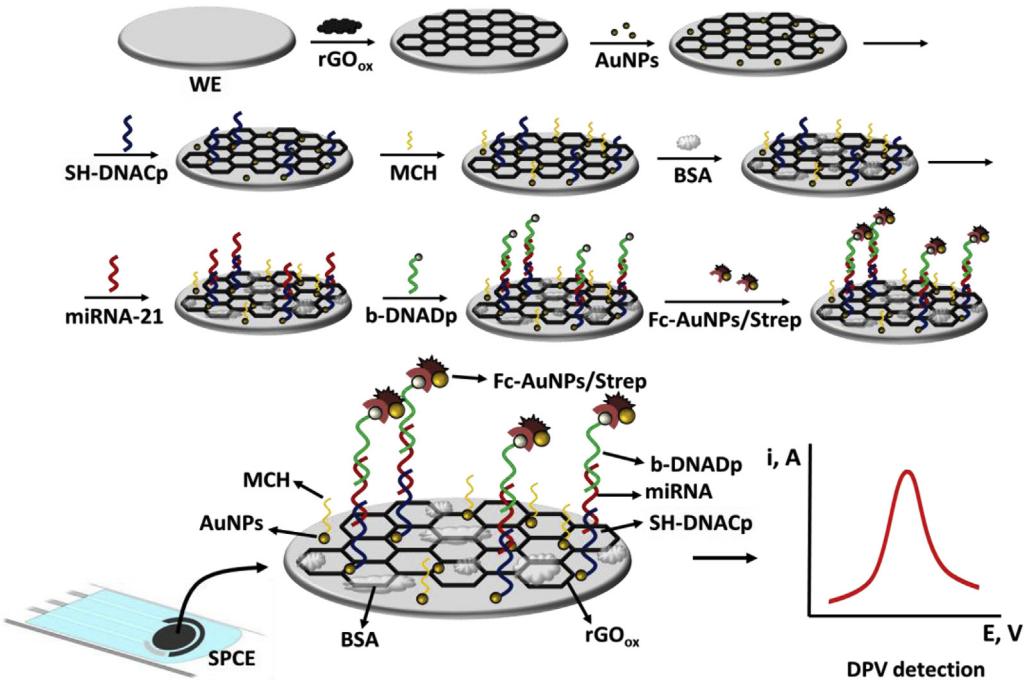

Scheme 1. Schematic display of the different steps involved in the preparation of the biosensor for miRNA determination at a HS-DNACp-AuNPs/rGO/SPCE involving a sandwich hybridization format, a biotinylated DNA detection probe (b-DNADp), labeling with Fc-AuNPs-Strep conjugates and DPV detection of the ferrocene reporter.

thoroughly with water and drying with nitrogen, the electrode was treated with 10 μL of a 0.1 mM MCH aqueous solution (also in Tris–EDTA, pH 8.0) for 5 min and, thereafter, in 1% (w/v) BSA (in Tris–EDTA, pH 8.0) for 1 h.

2.6. Sandwich hybridization and labeling of the b–DNADp at the HS–DNACp–AuNPs/rGO/SPCE

A 10–μL aliquot of the synthetic target miRNA or the biological sample (heated and diluted serum or RNA_t extracted from cells, all in sterilized PBS, pH 7.5 solutions) was cast onto the modified WE and incubated at room temperature during 30 min. After washing with water and drying with nitrogen, the WE was incubated with 10 μL of a 0.05 μM b–DNADp solution (prepared in Tris–EDTA, pH 8.0) for 30 min to obtain the sandwich hybridized duplexes. After washing and drying, the WE was incubated with 10 μL of the Fc–AuNPs–Strep conjugates for 45 min and then thoroughly rinsed with water and dried under N_2 [8].

All the manipulations before the electrochemical measurements were made in a laminar flow cabinet to avoid RNAse contamination and prevent target miRNA degradation.

2.7. Electrochemical measurements

DPV measurements were recorded between −0.5 and + 0.6 V (vs. the Ag pseudo–reference electrode) at 10 mV s^{-1} by dropping a 50–μL aliquot of PBS (pH 7.5) on the SPCE covering the three electrodes area. Electrochemical impedance spectroscopy (EIS)

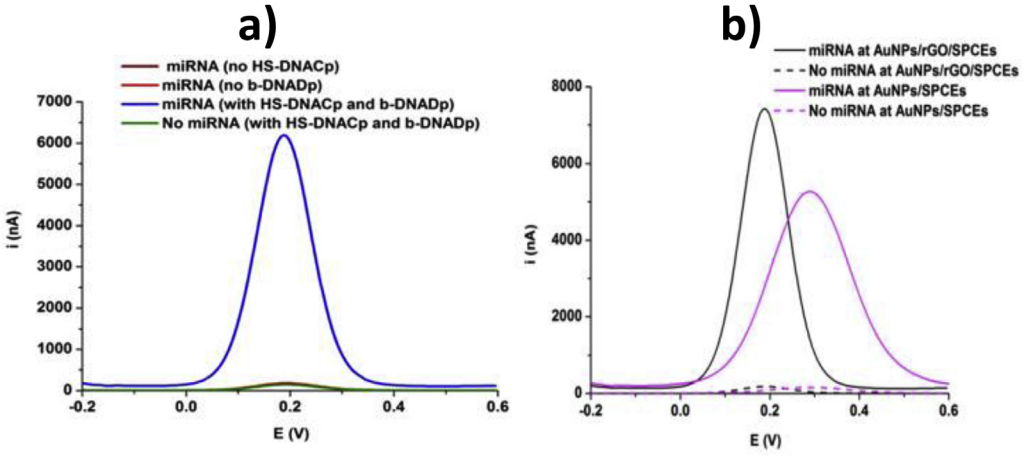

Fig. 1. a) DPV responses obtained in the absence and in the presence of 1 pM synthetic target miRNA–21 at HS–DNACp–AuNPs/rGO/SPCE, in the presence of 1 pM synthetic target miRNA–21 at AuNPs/rGO/SPCE and at HS–DNACp–AuNPs/rGO/SPCE but in the absence of b–DNADp. **b)** DPV responses recorded in the absence and in the presence of 1 pM synthetic target miRNA–21 with biosensors prepared at AuNPs/rGO/SPCEs and AuNPs/SPCEs. DPV recorded in PBS (pH 7.0).

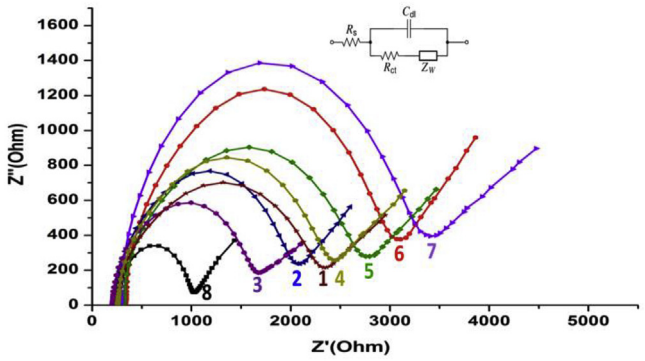

Fig. 2. Nyquist plots and Randles equivalent circuit (used to fit the experimental data) recorded at the different steps involved in the enzymeless biosensor preparation: bare SPCE (1), rGO/SPCE (2), AuNPs/rGO/SPCE (3), HS–DNACp–AuNPs/rGO/SPCE (4), MCH/HS–DNACp–AuNPs/rGO/SPCE (5), miRNA/MCH/HS–DNACp–AuNPs/rGO/SPCE (6), b–DNADp/miRNA/MCH/HS–DNACp–AuNPs/rGO/SPCE(7) and Fc–AuNPs–Strep/b–DNADp/miRNA/MCH/HS–DNACp–AuNPs/rGO/SPCE (8). 5 mM $[Fe(CN)_6]^{3-/4-}$ in 0.1 M KCl solution.

measurements were performed, upon placing a 50–μL drop of a 5 mM $[Fe(CN)_6]^{3-/4-}$ solution supplemented with 0.1 M KCl on the SPCE, over the 0.01–10,000 Hz frequency range with a 0.01 V rms signal at +0.12 V (vs. Ag–pseudo–reference electrode).

2.8. Determination of miRNA–21 in serum and RNA_t extracted from breast cells

The developed biosensor was applied to the determination of the endogenous miRNA–21 content in RNA_t extracted from breast cells (both epithelial non–tumorigenic and tumorigenic) and directly in human serum samples (without previous RNA_t extraction) from healthy and BC patients.

Protocols used for cells culture and RNA_t extraction were described previously [30,31]. In brief, the cell lines were grown at 37 °C in a humidified atmosphere containing 5% CO_2 in the appropriate media: high–glucose DMEM (Dulbecco's modified Eagle's medium), supplemented with 10% fetal bovine serum, 100 U mL^{-1} penicillin, 100 μg mL^{-1} streptomycin and 2.5 mM L–glutamine (GIBCO–Invitrogen, Carlsbad, CA, USA) (MCF–7, human breast adenocarcinoma cells) or in high–glucose DMEM/Ham's Nutrient Mixture F12 (1:1) containing 2.5 mM L–glutamine, 5% horse serum (Gibco), 10 mg mL^{-1} human insulin (Sigma), 0.5 mg mL^{-1} hydrocortisone (Sigma), 10 ng mL^{-1} EGF and 100 ng mL^{-1} cholera toxin (QuadraTech Ltd.) (MCF–10A, nontumorigenic human breast epithelial cells).

RNA_t was isolated by washing the cells with PBS, scraping off and spinning down. After homogenizing the pellet for 5 min in Tri Reagent (Molecular Research Center, Inc.) at room temperature, extraction was carried out with chloroform and the RNA_t (in the upper aqueous phase) was precipitated with isopropanol and washed twice with 70% EtOH. The resulting pellet was dried out in a heating plate at 80 °C during 10 min and stored at −80 °C after dissolving in RNase–free water [31]. The quality and concentration of the extracted RNA_t was evaluated by measuring the absorbance at the appropriate wavelengths with an ND–1000 spectrophotometer.

Blood serum samples from healthy individuals and BC patients were collected by Prof. Loueslati team (Biology department, University of Tunis El Manar) from informed consenting patients according to ethical guidelines. To perform the determination with the biosensor, a serum aliquot was 2-times diluted in the sterilized PBS, pH 7.5, and heated for 15 min at 95 °C in a block heater to release the miRNAs from microparticles and exosomes [32]. Subsequently, a 10–μL aliquot of this diluted and heated serum sample was casted onto the HS–DNACp–AuNPs/rGO/SPCE and the same protocol detailed in section 2.6 for synthetic target miRNA determination was carried out.

3. Results and discussion

3.1. Design of the E–bioplatform

The fundamental behind the miRNA–21 determination with the developed enzyme–free biosensor is illustrated in Scheme 1. The AuNPs/rGO/SPCE was modified with a binary monolayer composed of a thiolated DNA capture probe (HS–DNACp), which hybridized just with half of the target miRNA, and MCH. The presence of the target miRNA led to the formation of the HS–DNACp/miRNA duplex and the subsequent capture of a biotinylated DNA detection probe (b–DNADp) designed to be complementary to the unhybridized half of the miRNA. The biotinylated sandwich HS–DNACp/miRNA/b–DNADp hybrids attached to the AuNPs/rGO/SPCE were labeled with Fc–AuNPs–Strep conjugates, and DPV detection was carried out using the large number of Fc as reporter molecules.

Fig. 1 compares the DPV responses recorded in the presence and in the absence of the target miRNA at HS–DNACp–AuNPs/rGO/SPCEs, in the presence of the target miRNA at AuNPs/rGO/SPCE (with no HS–DNACp immobilized) and in the presence of the target miRNA at HS–DNACp–AuNPs/rGO/SPCE, i.e. in the absence of b–DNADp. As it can be observed, only a significant DPV response was obtained in the presence of both the target miRNA and b–DNADp at the HS–DNACp–AuNPs/rGO/SPCE (blue curve in Fig. 1a). This behavior confirmed the usefulness of the proposed biosensor design which did not exhibit significant non–specific adsorptions of the target miRNA, b–DNADp and Fc–AuNPs–Strep conjugates.

The relevant role played by the nanomaterials used to construct the biosensing scaffold was demonstrated by comparing the voltammetric responses obtained in the absence (B) and in the presence (S) of 1 pM miRNA–21 with biosensors prepared at AuNPs/rGO/SPCE and AuNPs/SPCE (Fig. 1b). The biosensor prepared with both nanomaterials provided a larger and narrower DPV peak, occurring at a lower potential value, in the presence of the target miRNA. In addition, no significant differences were found for the responses obtained in the absence of the target miRNA. Indeed, the ratio values between the DPV peak currents in the presence, S, and in the absence, B, of miRNA–21, S/B ratio, were 35.2 and 26.3 with biosensors prepared at AuNPs/rGO/SPCE and AuNPs/SPCE, respectively. These results confirmed the better voltammetric performance of the AuNPs/rGO/SPCE nanostructured platform with respect to the AuNPs/SPCE due to the synergic effect of both nanomaterials and the conducting nature of the rGO [21].

The role of each component in the bioplatform was evaluated by EIS characterization of the surfaces obtained after each step involved in the biosensor preparation. Fig. 2 shows the corresponding Nyquist plots and the Randles equivalent circuit used to fit the experimental data. As expected, important decreases in the charge transfer resistance (R_{ct}) were observed when the SPCE (R_{ct} = 2.43 kΩ) was modified with rGO (R_{ct} = 2.01 kΩ) and AuNPs/rGO (R_{ct} = 1.63 kΩ) thus suggesting the synergistic contribution of the two conducting components used [20,21,33,34]. The enhanced electron transfer kinetics at the AuNPs/rGO/SPCE can be attributed to the presence of AuNPs on rGO, which act as small conduction pockets for the diffusion of charge from solution to the electrode surface [21,35]. These results were in good agreement with those obtained by CV (Fig. S1a in the Supporting Information). In addition, and as expected, successive increases in the R_{ct} values were

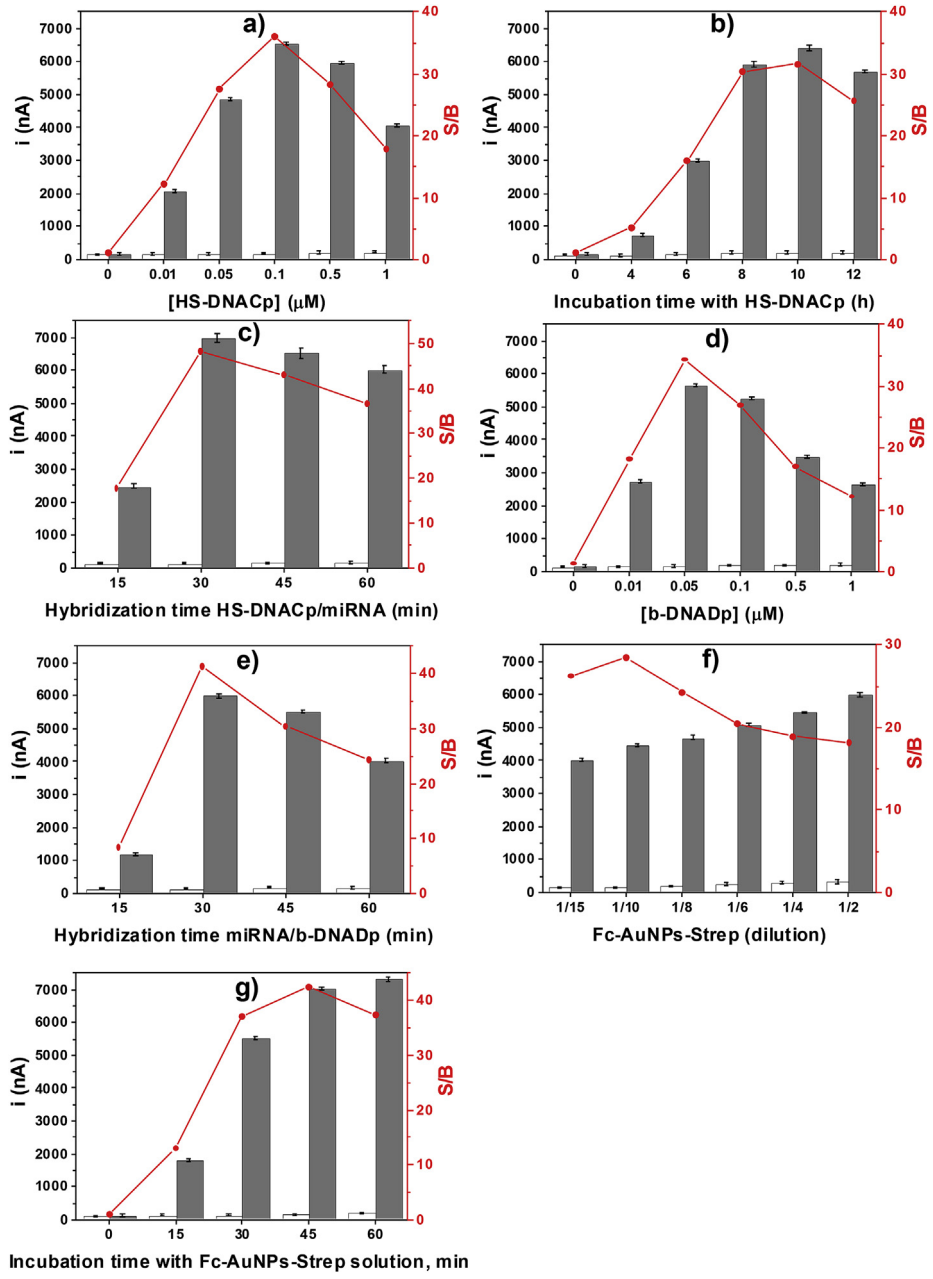

Fig. 3. Dependence of the DPV responses measured in the absence (white bars, B) and in the presence of 1 pM miRNA-21 (grey bars, S) and the corresponding S/B ratio (in red), with the: SH-DNACp concentration (a), incubation time with the SH-DNACp (b), SH-DNACp/miRNA hybridization time (c), b-DNADp concentration (d), miRNA/b-DNADp hybridization time (e), Fc-AuNPs-Strep solution dilution (f) and incubation time with the 10-times diluted Fc-AuNPs-Strep solution. Error bars were estimated as triple of the standard deviation (n = 3). (For interpretation of the references to colour in this figure legend, the reader is referred to the Web version of this article.)

observed after incubation with HS–DNACp (R_{ct} = 2.49 kΩ), MCH (R_{ct} = 2.89 kΩ), target miRNA (R_{ct} = 3.18 kΩ) and b–DNADp (R_{ct} = 3.48 kΩ), due to the insulating properties of these layers and the electrostatic repulsion between the redox probe and the negatively–charged immobilized oligonucleotides. Labeling of the b–DNADp with Fc–AuNPs–Strep conjugates resulted in a dramatic reduction of the R_{ct} (1.01 kΩ) because the attached conjugates make the external redox probe, $[Fe(CN)_6]^{3/4-}$ molecules, more accessible to the electrode surface [23]. It is worth to remark also that the short length of the sandwich hybrid (just 22 base pairs) allowed positioning the Fc moieties in closer vicinity of the underlying electrode to undergo faster electron transfer reaction [16].

3.2. Optimization of the experimental variables

The influence of all the experimental variables involved in the biosensor preparation on the responses obtained in the absence (B) and the presence (S) of 1 pM of the target synthetic miRNA was tested. The resulting S/B ratio was taken as a criterion for selecting the optimal conditions to ensure that the selected conditions minimized the possible nonspecific adsorptions.

Fig. 3 shows the results obtained in these optimization studies. It is important to note that most of the variables, with the exception of the dilution factor and incubation time with Fc–AuNPs–Strep, only exerted a significant influence on the specific responses obtained in the presence of the target miRNA. The results obtained

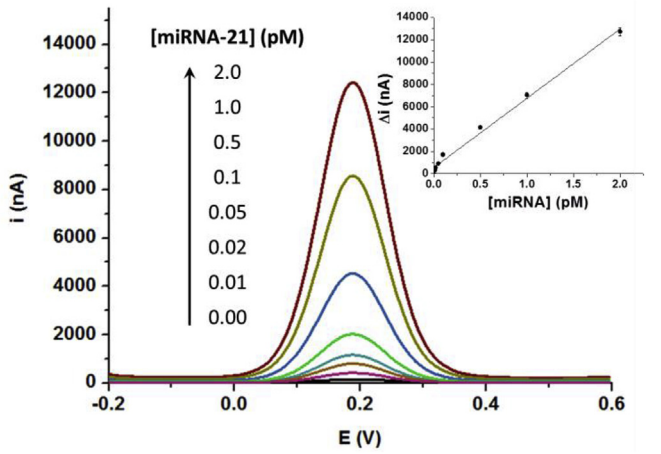

Fig. 4. DPV responses recorded with MCH/HS–DNACp–AuNPs/rGO/SPCEs under the optimized conditions for different miRNA–21 concentrations. Inset: linear calibration plot. Error bars estimated as triple of the standard deviation of three replicates.

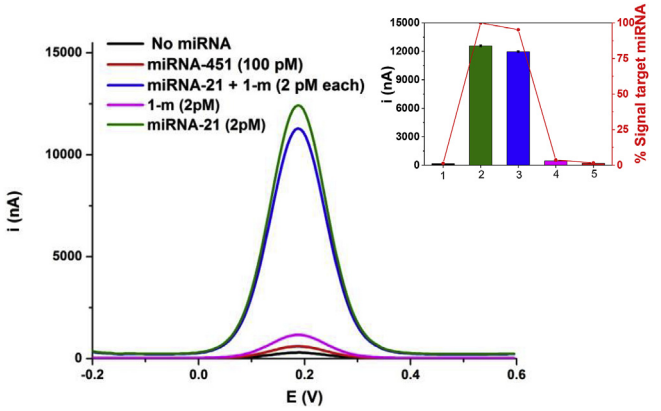

Fig. 5. Selectivity of the biosensor for target miRNA–21. DPV responses (and % signal given in comparison with the target miRNA in the inset) recorded in the absence of target miRNA (blank signal, bar 1 in inset) and in the presence of miRNA–21 (2 pM, bar 2 in inset), 1–m (2 pM, bar 4 in inset), NC (100 pM, bar 5 in inset) and a mixture solution containing miRNA–21/1–m (2 pM each, bar 3 in inset) synthetic sequences.

show as higher S/B ratios were achieved with a concentration and incubation time of 0.1 M (Figs. 3a) and 8 h (Fig. 3b), respectively, for the self–assembly of HS–DNACp on AuNPs/rGO/SPCE. The optimal hybridization time with the target miRNA was 30 min (Fig. 3c) as well as that of the hybridization with the b–DNACp (Fig. 3e). The responses obtained in the presence of miRNA–21 increased with the b–DNACp concentration until 0.05 μM, decreasing for larger concentrations (Fig. 3d) most likely due to the restricted hybridization efficiency when large amounts of the probe are used [36,37]. Regarding the variables involved in the labeling of the biotinylated sandwich hybrids with Fc–AuNPs–Strep, Fig. 3f and g shows that larger S/B ratio values were found by incubating over the electrode a 10 times–diluted dispersion for 45 min. Larger concentrations and longer incubation times provoked that the responses obtained in the absence of the target miRNA increased significantly more than in its presence and, consequently, the S/B ratio decreased. These results can be attributed to the slight increase in nonspecific adsorption of Fc-AuNPs-Strep when higher dispersion concentrations or longer incubation times are used. As expected, according to the rationale of the developed biosensor, it was not feasible to detect the target miRNA with biosensors prepared in the absence of HS–DNACp, b-DNADp or Fc–AuNPs–Strep (see bars at 0 in Fig. 3a, d and 3g). Table S1 in the Supporting Information summarizes the evaluated ranges of the experimental variables as well as the selected values for further work.

3.3. Analytical performance

Fig. 4 shows the calibration plot constructed from the DPV responses of the biosensor for the determination of miRNA–21. As it is shown in Fig. 4 inset, the Δ*i* value (calculated as the difference between the DPV peak current values measured in the presence and in the absence of each miRNA–21 concentration and used instead of i value to make the calibration line to pass through the origin) was linear (r = 0.992) with the miRNA–21 concentration from 10 fM to 2 pM. A LOD of 5 fM miRNA–21 (0.05 attomol in 10 μL sample) was estimated as three times the standard deviation of the DPV current values obtained for 10 independent measurements in the absence of miRNA–21.

The reproducibility of the used protocols and the storage stability of the prepared bioplatforms were also evaluated. A relative standard deviation (RSD) value of 3.9% was calculated from the DPV responses for 1 pM miRNA–21 provided by 10 different biosensors prepared in the same manner. This RSD confirmed the robustness of the protocols involved in the biosensor preparation and the voltammetric measurement. The storage stability was tested by preparing different MCH/HS–DNACp–AuNPs/rGO/SPCEs (after MCH treatment) and stored at 4 °C and in a humid environment. The responses provided by the stored biosensors for 0.05 pM miRNA–21, and also in the absence of miRNA, were recorded each control day. The results obtained are shown in Fig. S2 in the Supporting Information, where it can be observed as that the stored biosensors provided similar results for at least 63 days (no longer times were assayed). This prolonged storage stability, also demonstrated by other electrochemical bioplatforms reported for miRNAs implemented at AuNPs-modified SPCEs, could be attributed to the great biocompatibility of AuNPs, essential to keep the biological activity of the biomolecules attached to their surface [10,12,13].

3.4. Selectivity

The selectivity of the developed biosensor was evaluated by recording the DPV responses in the absence and in the presence of the target miRNA, and in the presence of synthetic sequences that differ in a single base (1–m) or are fully non complementary (NC) with respect to miRNA–21. The response obtained for a mixture containing miRNA–21 and the 1–m sequence at the same concentration was also checked.

Fig. 5 shows that no significant DPV responses were obtained in the presence of the NC (at a 50–times higher concentration) and 1–m sequences, thus allowing fully single nucleotide polymorphism (SNP) discrimination. In addition, Fig. 5 also shows that in the unlikely event the target miRNA was in the presence of a homologous miRNA with a single mismatched base in the same concentration [38], a similar response to that obtained for the target miRNA alone was obtained (Δ*i* values of 12,332 for miRNA–21 and 11,715 nA for the miRNA–21/1–m mixture solution).

This almost total discrimination towards the 1–m sequence is most likely due to the use of a sandwich hybridization strategy involving two independent hybridization steps of the target miRNA with as little as 11 mer–synthetic probes.

Table 2
Integrated electrochemical biosensors involving amplification strategies for the determination of miRNA-21 reported in the last 3 years.

Electrode	Fundamentals	Technique	Linear range	LOD	Number of steps/Assay time, min	Sample (amount)	Selectivity	Storage stability	Ref.
AuE	Aptameric sensor combined with the use of a triple amplification strategy (exonuclease T7-assisted target recycling method + Y-shaped branching ds-DNA based on HCR + CuNCs	DPSV (Cu^{2+})	0.1 fM–10 pM	10 aM	4 steps/~5 h 20 min starting from the aptasensor (~12 h 30 min)	Spiked 10-fold diluted serum samples from healthy volunteers	Clear discrimination against NC miRNAs	–	[8]
SPCE	Adsorption of the target miRNA/bDNACp heterohybrid (previously isolated onto Strep-MBs) on AuNP–Fe_2O_3NC-modified SPCE	Chronocoulometry ($[Ru(NH_3)_6]^{3+}$/$[Fe(CN)_6]^{3-/4-}$)	100 fM –1.0 mM	100 fM	4 steps/~2 h starting from AuNP–Fe_2O_3NC-modified SPCE	RNA_t extracted from human ESCC cell lines	Clear discrimination against non-complementary miRNAs	–	[39]
AuNPs-SPCE	Competition between target miRNA and a synthetic b-miRNA sequence to hybridize with a SH-RNACp assembled on the AuNPs-SPCE and further labeling of the b-miRNA attached with Strep-HRP	Amperometry (H_2O_2/HQ)	100 fM–25.0 pM	25 fM	2 steps/~1 h 15 min starting from SH-RNACp-AuNPs-SPCE (~13 h)	RNA_t extracted from BC cells (50 ng)	Total discrimination towards a 1-m	SH-RNACp- AuNPs-SPCE: ≥ 3 months	[10]
GCE	Direct hybridization at a GCE modified with a specific DNACp by sulfonic acid deposition and subsequent chlorination	EIS ($[Fe(CN)_6]^{3-/4-}$)	10 fM–10 nM	20 fM	1 step/~30 min starting from DNACp-GCE (~2 h)	Spiked urine samples from 5 control subjects	1-m: 40%, 2-m: 64%, 3-m: 14% and NC: 10% of the response provided by the target miRNA	–	[40]
Au-SPE	Adsorption of the target miRNA (previously captured onto bDNACp-Strep-MBs) on the Au-SPE	DPV ($[Fe(CN)_6]^{3-/4-}$)	1.0 pM-10 nM	1 pM	3 steps/> 40 min	RNA_t extracted from exosomes derived from cancer cells (50 ng)	–	–	[41]
SPCE	Adsorption of the target miRNA/bDNACp heterohybrid (previously isolated onto Strep-MBs) on SPCE modified with GO/IO NPs	Chronocoulometry ($[Ru(NH_3)_6]^{3+}$/$[Fe(CN)_6]^{3-/4-}$)	1.0 fM-1.0 nM	1.0 fM	4 steps > 1.5 h starting from SPCE modified with GO/IO NPs	RNA_t extracted from ovarian cancer cells	Clear discrimination against non-complementary miRNAs	–	[42]
AuNPs-SPCE	Direct hybridization approach at SH-RNACp assembled on the AuNPs-SPCE and recognition of the RNA/miRNA homohybrid with the fusion viral protein MBP-p19 further conjugated with an HRP-labeled anti-MBP antibody	Amperometry (H_2O_2/HQ)	0.5–50 pM	142 fM	3 steps/~1 h starting from SH-RNACp-AuNPs-SPCE (~9 h 5 min)	RNA_t extracted from BC cells (50 ng)	1-m: 40% of the response obtained for the target miRNA	SH-RNACp-AuNPs-SPCE: ≥ 2 months	[12]
AuNPs-SPCE	Direct hybridization approach at SH-DNACp assembled on the AuNPs-SPCE and recognition of the DNA/miRNA heterohybrid with an $Ab_{DNA-RNA}$ further conjugated with a ProtA-polyHRP$_{40}$	Amperometry (H_2O_2/HQ)	0.096–25 pM	29 fM	2 steps/~1 h 30 min starting from SH-DNACp-AuNPs-SPCE (~9 h 5 min)	RNA_t extracted from extracted from BC cells (10 ng) and serum samples from BC patients (diluted 1/5)	1-m: 30% of the response obtained for the target miRNA	SH-DNACp-AuNPs-SPCE: ≥ 2 months	[13]
AuE	Direct hybridization at a Cp-TSP-modified AuE and specific cleaved of DNA-RNA heterohybrids by DSN. The TSPs designed recognized both the target miRNA and a G-quadruplex sequence with biocatalytic functions for H_2O_2 reduction combined with hemin	DPV (TMB/H_2O_2)	0.1 fM–0.1 pM	0.04 fM	1 step/1 h starting from hemin–G-quadruplex–TSPs–Au (~12 h 30 min)	Spiked 1% human serum samples	1-m: ~20% of the response provided by the target miRNA	hemin–G-quadruplex–TSPs–Au: 94.2% the original response after 2 weeks	[43]
AuE	Direct hybridization at DNACp immobilized onto	DPV (Fc)	0.1 pM –10.0 nM	79.8 fM	2 steps/~2 h 5 min starting from AuE/		1-m: ~84%, 2-m: ~57% of the	–	[44]

(*continued on next page*)

Table 2 (*continued*)

Electrode	Fundamentals	Technique	Linear range	LOD	Number of steps/Assay time, min	Sample (amount)	Selectivity	Storage stability	Ref.
	cross-shaped DNA origami nanostructures (AuE/chitosan/origami-DNACp)				chitosan/origami-DNACp (~16 h)	Spiked 1% human serum samples	response provided by the target miRNA		
SPCE	Sandwich hybridization approach developed at a AuNPs/rGO/SPCE involving an SH-DNACp a b-DNADp and Fc-AuNPs-Strep	DPV (Fc)	10 fM–2 pM	5 fM	3 steps/~1 h 45 min starting from Fc-AuNPs-Strep (~24 h) and HS-DNACp-AuNPs/rGO/SPCE (~9 h 35 min)	RNA_t extracted from BC cells (50 ng) and serum samples from BC patients (diluted 1/2)	1-m: ~4% of the response provided by the target miRNA	SH-DNACP-AuNPs/rGO/SPCE: $\geq$ 2 months	This work

$Ab_{DNA-RNA}$: antibody selective to DNA/RNA heterohybrids; AuE: gold electrode; AuNP–Fe_2O_3NC: gold-loaded nanoporous superparamagnetic iron oxide nanocubes; AuNPs: gold nanoparticles; b: biotin; BC: breast cancer; Cp: capture probe; CuNCs: Cu nanoclusters; Dp: detector probe; DPSV: differential pulse stripping voltammetry; DPV: differential pulse voltammetry; DSN: duplex-specific nuclease; EIS: electrochemical impedance spectroscopy; ESCC: oesophageal squamous cell carcinoma; Fc: ferrocene; Fc-AuNPs-Strep: AuNPs/Strep conjugates capped with 6-(ferrocenyl)hexanethiol; GCE: glassy carbon electrode; GO/IO NPs: graphene-oxide-loaded superparamagnetic iron oxide nanoparticles; HCR: hybridization chain reaction; HQ: hydroquinone; LOD: limit of detection; LSV: Linear sweep stripping voltammetry; 1-m: single-base mismatched sequence; MBs: magnetic beads; MBP: maltose binding protein; NC: non-complementary sequence; ProtA-polyHRP$_{40}$: Protein A from *Staphylococcus aureus* conjugated with a homopolymer containing 40 molecules of HRP; rGO: reduced graphene oxide; RNA_t: total RNA; SHCp: thiolated capture probe; SPCE: screen-printed carbon electrode; Strep-HRP: conjugate of Streptavidin-horseradish peroxidase; Strep-MBs: streptavidin-modified MBs; TMB: 3,3′,5,5′-tetramethylbenzidine; TSP: tetrahedral DNA nanostructure probe.

3.5. Comparison with other electrochemical biosensors reported for miRNA-21 determination

Table 2 compares the main analytical characteristics of the developed biosensor with those reported for other electrochemical integrated biosensors recently reported for the determination of miRNA-21. As it can be observed, it is remarkable that the developed biosensor exhibits one of the lowest LOD values, with the exception of the sensors reported by Wang et al. [8] and Lu et al. [43], which, conversely, required the use of multiple probes and specific nucleases. The excellent discrimination towards a single-base mismatched sequence (1-m: ~4% of the response provided by the target miRNA) and the long storage stability of at least 2 months are competitive advantages of the proposed bioplatforms. It is important to note that the combination of these two interesting features were shown previously only by the biosensor proposed by Zouari et al. [10] which had a fivefold higher LOD using an enzyme-label based approach. Therefore, the developed biosensor provides, as a remarkable advantage, a pretty combination of good sensitivity, selectivity and operational stability using an enzymeless approach, which makes it less expensive and less prone to irreproducibility due to variations in the enzyme activity because of temperature or pH changes. Table 2 shows that, with the exception of the biosensor reported by Islam et al. [42], the other enzyme-free biosensors [39–41,44] provided worse LOD values (20 fM to 1 pM). Those testing their response towards 1-m sequences, showed just an acceptable (40–84% of the response provided by the target miRNA) selectivity. Moreover, their storage stability was not evaluated. The better sensitivity exhibited by the proposed biosensor can be attributed to the double nanostructured electrode surface and the amplified voltammetric signal due to the large number of Fc moieties at the Fc–AuNPs–Strep conjugates (~127 Fc moieties per AuNP) and their close proximity to the underlying electrode [15,16,23]. It is worth to note also that, compared to the only electrochemical assay described to date for the determination of miRNAs using Fc-AuNPs-Strep and involving MBs [24], the biosensor described in this paper, although offering a slightly higher LOD (5 vs 0.14 fM), requires a test time more than two times shorter (1 h 45 min *vs*. 4 h), which together with its integrated format and high storage stability makes it very attractive for future implementation in POC devices.

3.6. Determination of the miRNA–21 endogenous content in breast cancer sera and cells collected from breast cancer patients

The developed biosensor was used for the determination of the

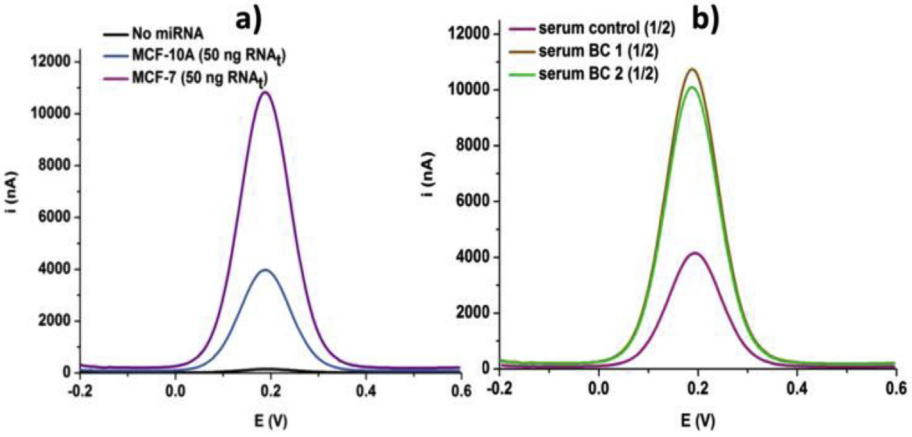

Fig. 6. DPV responses provided by the developed biosensors for the determination of the miRNA–21 endogenous content from 50 ng of RNA_t extracted from MCF–7 and MCF–10A cell lines (a) and 2–times diluted serum samples from a healthy volunteer and two different BC patients (b).

endogenous content of the oncogene miRNA–21 in RNA_t extracted from cells (breast adenocarcinoma MCF–7 cells and non–tumor MCF–10A epithelial cells) and directly in sera from BC patients and healthy subjects.

MiR-21 was assayed in the cells by analyzing 50 ng of cellular extracted RNA_t. This amount of genetic material was sufficient to perform the determination and, at the same time, ensured the absence of matrix effect. The slope values of the calibration plots constructed with miRNA–21 standards in the absence and in the presence of 50 ng RNA_t extracted from the MCF–10A epithelial breast cells, used as control, were 6209 ± 27 and 6633 ± 35 $nA \cdot pM^{-1}$, respectively ($t_{exp} = 3.068 < t_{tab} = 4.303$). Accordingly, the developed biosensor can provide quantitative data by simple interpolation of the measured DPV Δi (DPV traces are displayed in Fig. 6a) into the calibration plot for miRNA–21 standards (inset in Fig. 4). The results obtained are (0.95 ± 0.11) and (3.34 ± 0.17) amol miRNA–21 per ng of RNA_t in MCF–10A and MCF–7 cells, respectively, ($n = 3$, $\alpha = 0.05$). These endogenous contents are consistent with the oncogenic role of miRNA–21, with the 3–4 higher expression in the adenocarcinoma cell compared to the epithelial cell line [13,45,46] and with the concentrations reported by other authors [12,47–49].

Three serum samples (1 from a healthy individual and two from two different BC patients) were analyzed according to the protocol described in section 2.8. The recorded DPV traces (Fig. 6b) demonstrated that the expression of miRNA–21 is about 3 times higher for breast cancer patients than for healthy individuals, also in good agreement with previous results reported in breast tissues [45]. Moreover, no significant differences were found between the slope values of the calibration plot constructed with miRNA–21 standards in buffer solutions (between 10 fM and 1 pM) (Fig. 4 inset, (6209 ± 27 $nA \cdot pM^{-1}$)) or in 2 times–diluted serum of the healthy (6692 ± 25 $nA \cdot pM^{-1}$) ($t_{exp} = 3.127 < t_{tab} = 4.303$) and the BC patient (6604 ± 33 $nA \cdot pM^{-1}$) ($t_{exp} = 3.035 < t_{tab} = 4.303$) individuals. These results indicated that no significant matrix effect occurred also in the 2–times diluted serum, making it possible the determination of the miRNA–21 endogenous concentration in scarcely diluted serum samples without previous RNA_t extraction and by simple interpolation of the measured Δi values into the miRNA–21 standards calibration plot (inset in Fig. 4). The calculated miRNA–21 concentrations were (30 ± 5), (102 ± 7) and (89 ± 4) fM in healthy and BC patients 1 and 2 sera, respectively. It is worth noting here that the miRNA-21 expression found in serum, about 3–4 times larger in breast cancer patients that in healthy individuals, is in good agreement with reported results using an electrochemical biosensor [13] and a liquid chromatography–mass spectrometry (MS)/MS method [45].

These results demonstrate the possibility of accurate determination of the miRNA–21 endogenous content using directly scarcely diluted human blood serum and in a very small amount of cellular extracted RNA_t, without previous pre–concentration, amplification or reverse transcription to complementary DNA. However, it is important to mention that future efforts should focus on carrying out a more exhaustive validation comparing the results provided by this biosensor with a greater number of samples compared to conventional methodologies such as RT-qPCR.

4. Conclusions

This work reports the preparation of an enzyme–free biosensor for the sensitive and selective determination of miRNAs through the smart coupling of a sandwich hybridization assay, AuNPs/rGO-modified SPCEs to assemble the thiolated DNA capture probe, and Fc–AuNPs–Strep as nanotracers for labeling of the biotinylated DNA detector probe. Using as analytical readout the Fc DPV oxidation peak, the developed biosensors allowed achieving a LOD for the synthetic target miRNA down to low femtomolar level (5 fM) a full discrimination towards one mismatched base sequence and at least two months storage stability. This attractive performance is attributed to both the synergy in conducting and electrochemical properties of rGO and AuNPs in the AuNPs/rGO composite, which enhances the electron transfer rate, and the voltammetric signal amplification provided by the Fc–AuNPs–Strep. The biosensors demonstrated also their practical applicability for the determination of the target miRNA–21 endogenous content in breast adenocarcinoma cells and in 2–times diluted serum of breast cancer patients (without prior extraction of RNA_t), requiring only 50 ng of cellular RNA_t and 5 μL of serum sample per determination. The versatility of the developed strategy makes it potentially applicable for the determination of a wide variety of clinically relevant DNA or RNA biomarkers for other human cancers and chronic diseases simply by changing the synthetic capture and detection DNA probes. In addition, the facts that it does not use enzymes, whose activity can be affected by variations in pH and temperature causing irreproducibility problems, and that it provides quantitative readout of circulating miRNAs without previous extraction, amplification or reverse transcription to cDNA, portend the promising role of the developed strategy for implementation in POC devices usable in non–laboratory settings.

Declaration of competing interest

The authors declare that they have no known competing financial interests or personal relationships that could have appeared to influence the work reported in this paper.

CRediT authorship contribution statement

Mohamed Zouari: Investigation, Data curation, Writing - original draft. **Susana Campuzano:** Writing - review & editing, Funding acquisition. **José M. Pingarrón:** Writing - review & editing, Funding acquisition. **Noureddine Raouafi:** Conceptualization, Project administration, Supervision, Writing - review & editing, Funding acquisition.

Acknowledgment

University of Tunis El Manar is acknowledged for the mobility grant (Bourse d'Alternance) awarded to MZ and the Tunisian Ministry of Higher Education and Scientific Research (Lab. LR99ES15). NR thanks NanoFastResponse (PRF2017-D4P1) for financial support and Prof. Besma Loueslati (University of Tunis El Manar, Biology department) for the providing the serum samples used in the study. Spanish Ministerio de Economía y Competitividad Research Project, CTQ2015–64402–C2–1–R and the TRANSNANOAVANSENS–CM Program from the Comunidad de Madrid (Grant S2018/NMT–4349) are gratefully acknowledged. The authors would also like to acknowledge Drs. J.M. Sánchez–Puelles and E. López–Hernández for kindly providing us the RNA_t samples extracted from cell lines.

Appendix A. Supplementary data

Supplementary data to this article can be found online at https://doi.org/10.1016/j.aca.2020.01.016.

References

[1] P. Gillespie, S. Ladame, D. O'Hare, Molecular methods in electrochemical microRNA detection, Analyst 144 (2019) 114–129.

[2] M.N. Islam, M.K. Masud, N.T. Nguyen, V. Gopalan, H.R. Alamri, Z.A. Alothman, M.S. Al Hossain, Y. Yamauchi, A.K. Lamd, M.J.A. Shiddiky, Gold–loaded nanoporous ferric oxide nanocubes for electrocatalytic detection of microRNA at attomolar level, Biosens. Bioelectron. 101 (2018) 275–281.
[3] Y.X. Chen, K.J. Huang, K.X. Niu, Recent advances in signal amplification strategy based on oligonucleotide and nanomaterials for microRNA detection–a review, Biosens. Bioelectron. 99 (2018) 612–624.
[4] S. Campuzano, P. Yáñez–Sedeño, J.M. Pingarrón, Pushing the limits of electrochemistry toward challenging applications in clinical diagnosis, prognosis, and therapeutic action, ChemElectroChem 6 (2019) 60–72.
[5] P. Miao, Y. Tang, Q. Zhang, B. Bo, J. Wang, Identification of cellular MicroRNA coupling strand displacement polymerization and nicking-endonuclease-based cleavage, ChemPlusChem 80 (2015) 1712–1715.
[6] P. Miao, B. Wang, F. Meng, J. Yin, Y. Tang, Ultrasensitive detection of microRNA through rolling circle amplification on a DNA tetrahedron decorated electrode, Bioconjug. Chem. 26 (2015) 602–607.
[7] X. Wu, Y. Chai, R. Yuan, Y. Zhuo, Y. Chen, Dual signal amplification strategy for enzyme–free electrochemical detection of microRNAs, Sens. Actuators B Chem. 203 (2014) 296–302.
[8] Y. Wang, X. Zhang, L. Zhao, T. Bao, W. Wen, X. Zhang, S. Wang, Integrated amplified aptasensor with in–situ precise preparation of copper nanoclusters for ultrasensitive electrochemical detection of microRNA 21, Biosens. Bioelectron. 98 (2017) 386–391.
[9] D. Voccia, M. Sosnowska, F. Bettazzi, G. Roscigno, E. Fratini, V. De Franciscis, I. Palchetti, Direct determination of small RNAs using a biotinylated polythiophene impedimetric genosensor, Biosens. Bioelectron. 87 (2017) 1012–1019.
[10] M. Zouari, S. Campuzano, J.M. Pingarrón, N. Raouafi, Competitive RNA–RNA hybridization–based integrated nanostructured–disposable electrode for highly sensitive determination of miRNAs in cancer cells, Biosens, Bioelectron 91 (2017) 40–45.
[11] E. Vargas, E. Povedano, V. Ruiz–Valdepeñas Montiel, R.M. Torrente–Rodríguez, M. Zouari, J.J. Montoya, N. Raouafi, S. Campuzano, J.M. Pingarrón, Single–step incubation determination of miRNAs in cancer cells using an amperometric biosensor based on competitive hybridization onto magnetic beads, Sensors 18 (2018) 863.
[12] M. Zouari, S. Campuzano, J.M. Pingarrón, N. Raouafi, Ultrasensitive determination of microribonucleic acids in cancer cells with nanostructured–disposable electrodes using the viral protein p19 for recognition of ribonucleic acid/microribonucleic acid homoduplexes, Electrochim. Acta 262 (2018) 39–47.
[13] M. Zouari, S. Campuzano, J.M. Pingarrón, N. Raouafi, Amperometric biosensing of miRNA–21 in serum and cancer cells at nanostructured platforms using Anti–DNA–RNA hybrid antibodies, ACS Omega 3 (2018) 8923–8931.
[14] S. Campuzano, P. Yánez–Sedeño, J.M. Pingarrón, Electrochemical biosensing of microribonucleic acids using antibodies and viral proteins with affinity for ribonucleic acid duplexes, Electrochim. Acta 230 (2018) 271–278.
[15] J. Wang, J. Li, A.J. Baca, J. Hu, F. Zhou, W. Yan, D.W. Pang, Amplified voltammetric detection of DNA hybridization via oxidation of ferrocene caps on gold nanoparticle/streptavidin conjugates, Anal. Chem. 75 (2003) 3941–3945.
[16] A.J. Baca, F. Zhou, J. Wang, J. Hu, J. Li, J. Wang, Z.S. Chikneyan, Attachment of ferrocene-capped gold nanoparticle/streptavidin conjugates onto electrode surfaces covered with biotinylated biomolecules for enhanced voltammetric analysis, Electroanalysis 16 (2004) 73–80.
[17] L. Wu, E. Xiong, X. Zhang, X. Zhang, J. Chen, Nanomaterials as signal amplification elements in DNA–based electrochemical sensing, Nano Today 9 (2014) 197–211.
[18] L. Fritea, M. Tertis, R. Sandulescu, C. Cristea, Enzyme–graphene platforms for electrochemical biosensor design with biomedical applications, Methods Enzymol. 609 (2018) 293–333.
[19] Z. Zhu, L. Garcia–Gancedo, A.J. Flewitt, H. Xie, F. Moussy, W.I. Milne, A critical review of glucose biosensors based on carbon nanomaterials: carbon nanotubes and graphene, Sensors 12 (2012) 5996–6022.
[20] R. Singh, S. Hong, J. Jang, Label–free detection of influenza viruses using a reduced graphene oxide–based electrochemical immunosensor integrated with a microfluidic platform, Sci. Rep. 7 (2017) 42771.
[21] S. Verma, A. Singh, A. Shukla, J. Kaswan, K. Arora, J. Ramirez–Vick, S.P. Singh, Anti–IL8/AuNPs–rGO/ITO as an immunosensing platform for noninvasive electrochemical detection of oral cancer, ACS Appl. Mater. Interfaces 9 (2017) 27462–27474.
[22] M. Pedrero, S. Campuzano, J.M. Pingarrón, Electrochemical (bio) sensing of clinical markers using quantum dots, Electroanalysis 29 (2017) 24–37.
[23] H. Lu, L. Wu, J. Wang, Z. Wang, X. Yi, J. Wang, W. Wang, Voltammetric determination of the Alzheimer's disease–related ApoE 4 gene from unamplified genomic DNA extracts by ferrocene–capped gold nanoparticles, Microchim. Acta. 185 (2018) 549.
[24] Z. Lu, H. Tang, D. Wu, Y. Xia, M. Wu, X. Yi, H. Li, J. Wang, Amplified voltammetric detection of miRNA from serum samples of glioma patients via combination of conducting magnetic microbeads and ferrocene-capped gold nanoparticle/streptavidin conjugates, Biosens. Bioelectron. 86 (2016) 502–507.
[25] J.C. Liao, M. Mastali, Y. Li, V. Gau, M.A. Suchard, J. Babbitt, D.A. Haake, Development of an advanced electrochemical DNA biosensor for bacterial pathogen detection, J. Mol. Diagn. 9 (2007) 158–168.
[26] C. Martin, C. Grgicak, The effect of repeated activation on screen–printed carbon electrode cards, ECS Trans. 61 (2014) 1–8.
[27] L. Chen, Y. Tang, K. Wang, C. Liu, S. Luo, Direct electrodeposition of reduced graphene oxide on glassy carbon electrode and its electrochemical application, Electrochem. Commun. 13 (2011) 133–137.
[28] W. Argoubi, M. Saadaoui, S. Ben Aoun, N. Raouafi, Optimized design of a nanostructured SPCE–based multipurpose biosensing platform formed by ferrocene–tethered electrochemically–deposited cauliflower–shaped gold nanoparticles, Beilstein J. Nanotechnol. 6 (2015) 1840–1852.
[29] Y. Hu, J. Jin, P. Wu, H. Zhang, C. Cai, Graphene–gold nanostructure composites fabricated by electrodeposition and their electrocatalytic activity toward the oxygen reduction and glucose oxidation, Electrochim. Acta 56 (2010) 491–500.
[30] S. Campuzano, R.M. Torrente-Rodríguez, E. López-Hernández, F. Conzuelo, R. Granados, J.M. Sánchez-Puelles, J.M. Pingarrón, Magnetobiosensors based on viral protein p19 for microRNA determination in cancer cells and tissues, Angew. Chem. Int. Ed. 53 (2014) 6168–6171.
[31] R.M. Torrente-Rodríguez, S. Campuzano, E. López-Hernández, R. Granados, J.M. Sánchez-Puelles, J.M. Pingarrón, Direct determination of miR-21 in total RNA extracted from breast cancer samples using magnetosensing platforms and the p19 viral protein as detector bioreceptor, Electroanalysis 26 (2014) 2080–2087.
[32] M. Labib, N. Khan, S.M. Ghobadloo, J. Cheng, J.P. Pezacki, M.V. Berezovski, Three–mode electrochemical sensing of ultralow microRNA levels, J. Am. Chem. Soc. 135 (2013) 3027–3038.
[33] S. Singh, S.K. Tuteja, D. Sillu, A. Deep, C.R. Suri, Gold nanoparticles–reduced graphene oxide based electrochemical immunosensor for the cardiac biomarker myoglobin, Microchim. Acta. 183 (2016) 1729–1738.
[34] V. Serafín, R.M. Torrente–Rodríguez, A. González–Cortés, P.G. de Frutos, M. Sabaté, S. Campuzano, J.M. Pingarrón, An electrochemical immunosensor for brain natriuretic peptide prepared with screen–printed carbon electrodes nanostructured with gold nanoparticles grafted through aryl diazonium salt chemistry, Talanta 179 (2018) 131–138.
[35] K. Saha, S.S. Agasti, C. Kim, X. Li, V.M. Rotello, Gold nanoparticles in chemical and biological sensing, Chem. Rev. 112 (2012) 2739–2779.
[36] M.A. Pereira–Barros, M.F. Barroso, L. Martín–Pedraza, E. Vargas, S. Benedé, M. Villalba, J.M. Pingarrón, Direct PCR–free electrochemical biosensing of plant–food derived nucleic acids in genomic DNA extracts. Application to the determination of the key allergen Sola l 7 in tomato seeds, Biosens. Bioelectron. 137 (2019) 171–177.
[37] S. Liu, Y. Lin, T. Liu, C. Cheng, W. Wei, L. Wang, F. Li, Enzyme–free and label–free ultrasensitive electrochemical detection of DNA and adenosine triphosphate by dendritic DNA concatamer–based signal amplification, Biosens. Bioelectron. 56 (2014) 12–18.
[38] F. Li, J. Peng, J. Wang, H. Tang, L. Tan, Q. Xie, S. Yao, Carbon nanotube–based label–free electrochemical biosensor for sensitive detection of miRNA–24, Biosens. Bioelectron. 54 (2014) 158–164.
[39] M.K. Masud, N. Islam, H. Haque, S. Tanaka, V. Gopalan, G. Alici, N.-T. Nguyen, A.K. Lam, S.A. Hossain, Y. Yamauchi, M.J.A. Shiddiky, Gold-loaded nanoporous superparamagnetic nanocubes for catalytic signal amplification in detecting miRNA, Chem. Commun. 53 (2017) 8231–8234.
[40] D.A. Smith, L.J. Newbury, G. Drago, T. Bowen, J.E. Redman, Sens. Actuators B Chem. 253 (2017) 335–341.
[41] K. Boriachek, M. Umer, M.N. Islam, V. Gopalan, A.K. Lam, N.T. Nguyen, M.J.A. Shiddiky, An amplification-free electrochemical detection of exosomal miRNA-21 in serum samples, Analyst 143 (2018) 1662–1669.
[42] N. Islam, L. Gorgannezhad, M.K. Masud, S. Tanaka, S.A. Hossain, Y. Yamauchi, N.-T. Nguyen, M.J.A. Shiddiky, Graphene-oxide-loaded superparamagnetic iron oxide nanoparticles for ultrasensitive electrocatalytic detection of microRNA, ChemElectroChem 5 (2018) 2488–2495.
[43] J. Lu, J. Wang, X. Hu, E. Gyimah, S. Yakubu, K. Wang, X. Wu, Z. Zhang, Electrochemical biosensor based on tetrahedral DNA nanostructures and G-quadruplex–hemin conformation for the ultrasensitive detection of microRNA-21 in serum, Anal. Chem. 91 (2019) 7353–7359.
[44] S. Han, W. Liu, S. Yang, R. Wang, Facile and label-free electrochemical biosensors for microRNA detection based on DNA origami nanostructures, ACS Omega 4 (2019) 11025–11031.
[45] L. Liu, Q. Xu, S. Hao, Y. Chen, A quasi–direct LC–MS/MS–based targeted proteomics approach for miRNA quantification via a covalently immobilized DNA–peptide probe, Sci. Rep. 7 (2017) 5669.
[46] L.X. Yan, X.F. Huang, Q. Shao, M.Y. Huang, L. Deng, Q.L. Wu, J.Y. Shao, MicroRNA miR–21 overexpression in human breast cancer is associated with advanced clinical stage, lymph node metastasis and patient poor prognosis, RNA 14 (2008) 2348–2360.
[47] F. Xu, T. Yang, Y. Chen, Quantification of microRNA by DNA–Peptide probe and liquid chromatography–tandem mass spectrometry–based quasi–targeted proteomics, Anal. Chem. 88 (2015) 754–763.
[48] R.M. Torrente–Rodríguez, V. Ruiz–Valdepeñas Montiel, S. Campuzano, M. Farchado–Dinia, R. Barderas, P. San Segundo–Acosta, J.M. Pingarron, Fast electrochemical miRNAs determination in cancer cells and tumor tissues with antibody–functionalized magnetic microcarriers, ACS Sens. 1 (2016) 896–903.
[49] E. Vargas, R. Torrente–Rodríguez, V. Ruiz–Valdepeñas Montiel, E. Povedano, M. Pedrero, J. Montoya, J.M. Pingarrón, Magnetic beads–based sensor with tailored sensitivity for rapid and single–step amperometric determination of miRNAs, Int. J. Mol. Sci. 18 (2017) 2151.